

Crystal Structures of the Ribosome in Complex with Release Factors RF1 and RF2 Bound to a Cognate Stop Codon

Sabine Petry,¹ Ditlev E. Brodersen,^{1,2} Frank V. Murphy IV,¹ Christine M. Dunham,¹ Maria Selmer,¹ Michael J. Tarry,^{1,3} Ann C. Kelley,¹ and V. Ramakrishnan^{1,*}

¹MRC Laboratory of Molecular Biology, Hills Road, Cambridge CB2 2QH, United Kingdom

²Present Address: Department of Molecular Biology, University of Aarhus, Gustav Wieds Vej 10c, DK-8000 Aarhus C, Denmark.

³Present Address: Department of Biochemistry, University of Oxford, South Parks Road, Oxford OX1 3QU, United Kingdom.

*Contact: ramak@mrc-lmb.cam.ac.uk

DOI 10.1016/j.cell.2005.09.039

SUMMARY

During protein synthesis, translational release factors catalyze the release of the polypeptide chain when a stop codon on the mRNA reaches the A site of the ribosome. The detailed mechanism of this process is currently unknown. We present here the crystal structures of the ribosome from *Thermus thermophilus* with RF1 and RF2 bound to their cognate stop codons, at resolutions of 5.9 Å and 6.7 Å, respectively. The structures reveal details of interactions of the factors with the ribosome and mRNA, including elements previously implicated in decoding and peptide release. They also shed light on conformational changes both in the factors and in the ribosome during termination. Differences seen in the interaction of RF1 and RF2 with the L11 region of the ribosome allow us to rationalize previous biochemical data. Finally, this work demonstrates the feasibility of crystallizing ribosomes with bound factors at a defined state along the translational pathway.

INTRODUCTION

During the elongation phase of protein synthesis, triplet codons on mRNA are decoded on the ribosome by their cognate aminoacyl tRNAs, resulting in addition of amino acids to the growing polypeptide chain. This process continues until a stop codon is presented in the A site of the 30S ribosomal subunit, signifying the end of the coding sequence for a particular gene. The triplets UAG, UGA, or UAA act as stop codons in almost all species. Stop codons are decoded not by a tRNA but by proteins known as class I release factors

(RFs) (Capecchi, 1967; Caskey et al., 1968; Scolnick et al., 1968). In prokaryotes, the three stop codons are recognized by two proteins with overlapping specificities: RF1, which recognizes UAG and UAA, and RF2, which recognizes UGA and UAA (Scolnick et al., 1968). Eukaryotes, archaea, and mitochondria possess a single class I RF, termed eRF1, aRF1, and mtRF1, respectively, which recognizes all three stop codons (Konecki et al., 1977). Eukaryotic and archaeal release factors are more similar to each other in sequence and are relatively distinct from their bacterial counterparts (Frolova et al., 1999).

Upon stop-codon recognition, class I RFs promote hydrolysis of the ester bond that links the nascent polypeptide chain with the tRNA in the P site, leading to release of the polypeptide chain from the ribosome (Capecchi, 1967; Caskey et al., 1968; Scolnick et al., 1968). Subsequently, the release of the bound class I RF from the ribosome is facilitated by RF3, a class II release factor, which is a GTPase like many of the other protein factors involved in translation. It has been proposed that the ribosome-class I RF complex promotes GDP-to-GTP exchange in RF3 only after polypeptide release (Zavialov et al., 2001). Nucleotide exchange is followed by release of RF1 or RF2 from the ribosome. Finally, GTP hydrolysis by RF3 results in its own release.

Two key unresolved questions concerning RF function are (1) how are stop codons recognized specifically by a protein, and (2) how does this result in release of the polypeptide chain from P site tRNA? Discrimination between stop and sense codons by RFs is achieved without the proofreading used in tRNA selection (Freistroffer et al., 2000). Genetic experiments have shown that it is possible to switch the specificity of RF1 and RF2 by swapping a tripeptide motif within each factor, P(A/V)T in RF1 and SPF in RF2 (Ito et al., 2000). This led to the suggestion that a tripeptide “anticodon” may be involved in direct recognition of the stop codon.

However, the situation may be somewhat more complicated for several reasons. First, bases that are both downstream (Poole et al., 1995) and upstream (Mottagui-Tabar, 1998) of the stop codon seem to affect termination efficiency. Second, the ribosome itself may be involved in decoding of stop codons since mutations in both 16S and 23S ribosomal

RNA result in readthrough of stop codons in vivo (reviewed in Arkov and Murgola, 1999). Finally, mutations elsewhere in RF2 within the domain containing the tripeptide motif, in which lysine residues are exchanged for glutamic-acid residues, can trigger polypeptide release at noncognate stop codons as well as sense codons (Ito et al., 1998; Uno et al., 2002).

The only sequence motif universally conserved in all known class I RFs is the GGQ motif (Frolova et al., 1999). It is likely to be involved in the hydrolytic activity of RFs by a yet unknown mechanism since its mutation greatly reduces the ability of RFs to stimulate peptidyl-tRNA hydrolysis but does not affect ribosome binding in either eukaryotes (Frolova et al., 1999; Song et al., 2000; Seit-Nebi et al., 2001) or prokaryotes (Zavialov et al., 2002; Mora et al., 2003). The glutamine residue of the conserved GGQ motif of *E. coli* RF1 and RF2 and yeast eRF1 is methylated at the N5 position (Dincbas-Renqvist et al., 2000; Heurgue-Hamard et al., 2005). The absence of this methylation decreases the in vitro release activity of *E. coli* RF2 by several-fold.

Mutational studies suggest a role for ribosomal RNA in peptidyl-tRNA hydrolysis. In one study, it was concluded that, of four conserved residues at the core of the peptidyl transferase center (PTC) of the 50S subunit, A2451, U2585, and C2063 do not significantly affect the reaction, whereas mutations of A2602 dramatically impede peptide release but have little effect on peptide-bond formation (Polacek et al., 2003). However, more recent kinetic analysis on affinity-purified mutant ribosomes showed that mutations of these same residues all affect peptide release to varying degrees but have little effect on peptide-bond formation (Youngman et al., 2004).

In addition to their codon specificities, another major difference between RF1 and RF2 appears to be in their interactions with the L11 region of the ribosome. It has been shown that, with ribosomes lacking L11, RF1 has significantly lower efficiency, but RF2 function is only somewhat inhibited (Tate et al., 1983; Van Dyke et al., 2002). A later study showed that it was the N-terminal domain of L11 that was responsible for the observed effect on termination (Van Dyke and Murgola, 2003). In contrast, mutations in the corresponding L11 binding region of 23S RNA affected RF2 but not RF1 function (Arkov et al., 1998).

The crystal structures of isolated RF1 and RF2 are similar (Vestergaard et al., 2001; Shin et al., 2004), as might be expected given the homology between the two factors, and are unlike the previously solved structure of eRF1 (Song et al., 2000). However, in the case of RF1 and RF2, the distance between the tripeptide motif that confers stop-codon specificity and the GGQ motif that is involved in peptide release is incompatible with the distance between the decoding center in the 30S subunit and the PTC in the 50S subunit. A model for RF2 binding to the ribosome was proposed based on its similarity with the shape of tRNA (Vestergaard et al., 2001), but this model was incompatible with a direct interaction between the tripeptide motif and the stop codon proposed earlier (Ito et al., 2000).

This discrepancy was resolved by two independent cryo-EM reconstructions of RF2 bound to a stop codon on the ri-

bosome (Klaholz et al., 2003; Rawat et al., 2003). In these structures, RF2 does not act as a strict structural mimic of tRNA. Rather, there appears to be a dramatic change in the relative orientation of the various domains in RF2 compared to the isolated crystal structure: When bound to the ribosome, the domain that contains the GGQ motif extends toward the PTC, whereas it is packed against the core of RF2 in the isolated crystal structure. This allowed a model in which the domain containing the tripeptide motif could be placed in the decoding center of the 30S subunit.

While the results from cryo-EM represented a major advance, it is clear that understanding the mode of action of RFs will require more detailed structures. For example, there are differences in the detailed conformation of RF2 between the two independent cryo-EM structures even though the two structures were determined from similar samples obtained from the same laboratory. Similar differences in the structure and interactions of EF-Tu and tRNA with the ribosome also arose in previous independent cryo-EM structures (Stark et al., 2002; Valle et al., 2002). These differences make it difficult to make detailed statements about interactions of various elements of RFs with the ribosome or conformational changes that cannot be resolved in medium-resolution cryo-EM maps.

There are fewer problems in interpretation when a threshold of about 7 Å resolution is reached. Beyond this resolution, protein α helices are apparent as tubes of electron density and β sheets as surfaces, while the RNA backbone is well resolved. This allows accurate placement of protein domains without reference to external constraints such as biochemical or genetic data. Such a resolution is now being approached in cryo-EM studies but is still far from routine. On the other hand, crystallization of programmed ribosomes with bound translational factors at specific points on the translational pathway has proven challenging, probably due to the difficulty of preparing a homogeneous and stable population of ribosomes in a defined state.

Here we report crystal structures of programmed ribosomes with P site tRNA; a cognate stop codon in the A site; and RF1 or RF2, at 5.9 Å and 6.7 Å resolution, respectively. We also report a structure at 6.4 Å of the corresponding complex without release factor. At this resolution, the secondary structure of all four RF domains can be clearly seen for both RF1 and RF2, allowing their unambiguous placement in electron density maps. The structures reveal details about the environment of the RFs in the decoding center and the PTC, changes in the L11 region in response to RF binding, and differences between RF1 and RF2 in this region. The results provide a more detailed understanding of the interactions of class I release factors with the ribosome.

RESULTS AND DISCUSSION

Formation of Homogeneous Release Complexes

Release complexes were formed with 70S ribosomes, leaderless mRNA, tRNA^{Phe} bound to a cognate codon in the P site, and an A site that was either empty (RC0) or contained specifically bound RF1 (RC1) or RF2 (RC2). Separation of

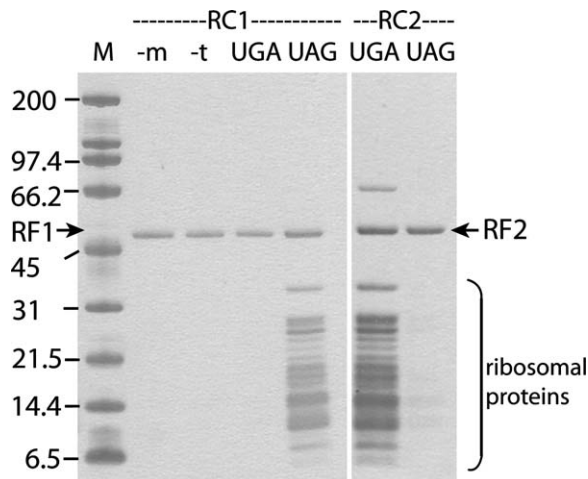


Figure 1. Codon-Specific Purification of Functional Complexes of the Ribosome with Release Factors by Affinity Tagging

Complexes were formed between ribosomes, mRNA with a Phe codon (UUC) in the P site and a stop codon in the A site (UAG or UGA), tRNA^{Phe}, and His-tagged RF1 or RF2; purified by affinity chromatography using Ni-NTA columns; and analyzed on SDS-PAGE. The gels show that stable complexes of release factors bound to ribosomes are formed only when cognate stop codons in the A site and P site tRNA are both present. The lanes indicate whether RF1 or RF2 was used, which codon was present in the A site, and whether either mRNA (–m) or tRNA (–t) was left out during complex formation. The additional band in the RF2 lanes is from ribosomal protein S1, which is not required for release-factor binding and was removed in the subsequent samples used for crystallization. The lane marked M shows molecular-weight markers.

functional complexes from the overall ribosome population was accomplished by affinity purification using a His tag on RF1 or RF2. Indeed, such affinity purification showed that stable binding of the RF to the A site depended on the presence of both mRNA and P site tRNA (Figure 1). These studies also showed that there is virtually no binding of RF1 with UGA or RF2 with UAG, indicating that the purified complexes of the ribosome contain a release factor bound specifically to a cognate stop codon. Since the P site tRNA used here is deacylated, the complexes represent the state after release of the peptide chain by RF.

Crystallization and Structure Determination

Despite significant effort, we were unable to reproduce the crystallization conditions for complexes of *T. thermophilus* 70S ribosomes with mRNA and tRNA reported previously (Cate et al., 1999), even when identical ligands were used. An extensive search for new crystallization conditions resulted in crystals in the space group P4₃2₁2 that diffracted to resolutions of up to 5.5 Å. The structure was solved by molecular replacement and refined (Table 1) as described in Experimental Procedures. Difference Fourier maps showed clear and continuous density for both P site tRNA and RF1 or RF2, when present (Figures 2A–2C). Homology models for *T. thermophilus* RF1 and RF2 were generated from the isolated crystal structures from *T. maritima* (Shin et al., 2004)

Table 1. Summary of Crystallographic Data

Data Set	RC0	RC1	RC2
Data Collection			
Unit cell dimensions			
a, b (Å)	517.4	519.0	519.9
c (Å)	365.4	365.1	364.8
Resolution (Å)	100–6.4 ^a	100–5.9 ^a	100–6.76 ^a
Number of crystals	4	3	5
Number of reflections	9,410,644	5,020,072	2,894,665
Observational			
redundancy	11.5	7.8	5.7
Completeness (%)	99.9	95.4	99.1
Mean I/σ(I)	10.1	11.3	8.2
R _{sym} (%)	13.1	13.4	19.3
Refinement with CNS			
Resolution (Å)	40–6.4	40–5.9	40–6.76
R _{free} (%) ^b	36.1	37.1	35.6
R _{work} (%)	35.4	35.1	34.1
Refinement with Refmac			
Resolution (Å)	40–6.0	40–5.5	40–6.0
R _{free} (%) ^b	37.7	38.0	38.0
R _{work} (%)	34.3	35.1	34.9
Figure of merit	0.69	0.66	0.68

^a Outer resolution represents value at which mean I/σ is 2.

^b Five percent of the reflections were used for crossvalidation.

and *E. coli* (Vestergaard et al., 2001), respectively, using the sequence alignment shown in Figure 3A. These homology models allowed an unambiguous fit of the factors without reference to prior biochemical or genetic data. As in previous crystal structures of the 70S ribosome (Yusupov et al., 2001), density was also seen for E site tRNA, which is presumably noncognate since only one species of tRNA was added to tRNA-free ribosomes.

Overall Description of RF1/2

In agreement with the previous cryo-EM results on RF2 bound to the ribosome (Klaholz et al., 2003; Rawat et al., 2003), both RF1 and RF2 exhibit an extended conformation compared to the isolated crystal structures: Domain 3 of each factor has peeled away from away from the core of RF consisting of domains 2 and 4 and extends into the PTC, whereas domain 2 makes contact with the decoding center (Figures 3B–3D). However, the two RF2 cryo-EM models differ significantly both from one another and from the crystal structure in the placement of structural elements, including the GGQ and tripeptide motifs (see Figure S1 in the Supplemental Data available with this article online), showing both the strengths and limitations of models based on medium-resolution cryo-EM maps. Moreover, at the resolution of the

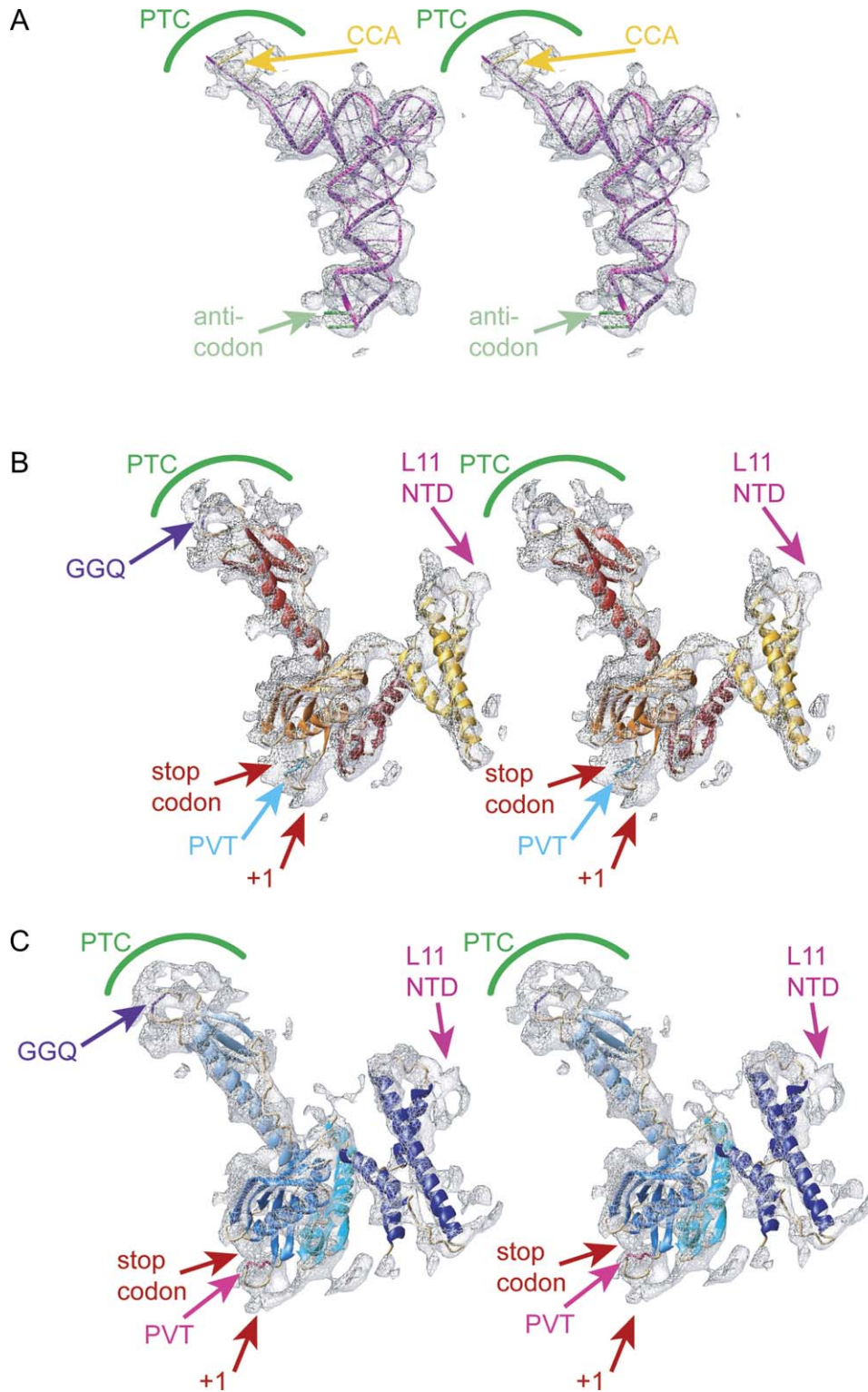


Figure 2. Difference Fourier Maps (in Stereo) of tRNA and Release Factors Bound to the Ribosome

The maps were masked around the molecule using a probe radius of 7 Å, at which comparison with unmasked maps showed that no artificial truncations were introduced in the density for the tRNA or factors. Because these maps were obtained prior to the inclusion of either ligands or factor in the model used for molecular replacement, they are unbiased. Electron density extending from the factors stems from interacting elements as indicated and referred to in the text. (A) $F_o - F_c$ map contoured at 2σ showing P site tRNA (violet) with the anticodon bases in green and the CCA bases in yellow.

crystal structures, several detailed interactions of RF with the ribosome now become apparent. In addition to the changes in the orientation of the domains, we also see induced conformational changes within and between domains in RF upon binding to the ribosome, as well as changes in the conformation of L11 in the ribosome.

Globally, the structures of RF1 and RF2 are similar. Domains 2 and 4 remain as a compact superdomain, as in the isolated crystal structures. The dimensions and location of the superdomain 2/4, which interacts with the decoding site, and domain 3 in the PTC taken together match that of A site tRNA (Figures 3D and 3E). Domain 1 of the RFs is more accessible and extends from the L11 region to the 30S beak. Its conformation, along with that of the C-terminal helix of domain 4, varies more between RF1 and RF2 (Figure S1D).

Most of the conformational changes in the RFs that are observed upon binding to the ribosome are in domain 3, which contains the GGQ motif. This domain flips out from the core of the protein in order to reach the PTC. Its long helix ($\alpha 7$) appears extended by several residues (RF1, 283–287; RF2, 297–303) compared to the isolated crystal structures. In contrast, the adjacent linker that connects domain 2 to domain 3 appears to be an extended polypeptide chain that is clearly defined in the electron density map. Interestingly, the loop between strands $\beta 6$ and $\beta 7$ containing the GGQ motif (residues 223–236 in RF1; 233–246 in RF2), which is highly mobile and not resolved in the isolated crystal structures, becomes ordered when it interacts with the PTC and is visible as a continuous loop of electron density in both structures (Figures 2B and 2C).

We also observe a rotation of domain 1 away from the 2/4 superdomain, which anchors it to the L11 region. In the isolated crystal structure, helix $\alpha 3$ of RF2 (residues 43–81) appears bent, unlike the corresponding helix in RF1, which is straight. This helix appears straight in both factors in complex with the ribosome.

Decoding

To date, the question of how class I RFs recognize stop codons has remained elusive. In the structures presented here, the RF region closest to the stop codon is the loop between strands $\beta 4$ and $\beta 5$ containing the putative tripeptide anticodon (PVT, 184–186 for RF1; SPF, 191–193 for RF2) (Ito et al., 2000). Intriguingly, the electron density for this loop region suggests that RF surrounds the anticodon, especially in the second and third position (Figure 4). All the residues in this loop are in close proximity to the A site codon. It was not possible to resolve the loop from the stop codon itself, presumably due to their close association. If one assumes that the loop is in approximately the same conformation as in the isolated crystal structures, then residues 184–187 and 191–193 (RF1 numbering) surround the stop codon, whereas residues 188–190 constitute the tip of the loop. This means

that the loop would have to change conformation upon binding to the ribosome for the tripeptide motif to be in direct contact with the stop codon. The electron density extends from the tip of this loop to the base just 3' of the stop codon (+1 in Figure 2, and 3' U in Figure 4), which is in accordance with the biochemical finding that this downstream base contributes to the decoding efficiency of the stop signal.

Interestingly, the uridine in the first position of the stop codon is flanked by the tip of helix $\alpha 5$ of the RFs (Figure 4). Thr115 and the highly conserved residues Glu118 and Glu119 (RF1 numbering) are in close proximity to this base, while Gly116 and Gly117 allow the sharp bend at the end of the helix. Whereas the tripeptide loop faces the stop-codon bases, the blunt tip of helix $\alpha 5$ is parallel to the plane of the first base.

Together, both of these elements in RF may act as molecular tweezers. The tip of helix $\alpha 5$ (common to RF1 and RF2) could discriminate against A, G, and C at position 1, and the anticodon loop (specific to RF1 or RF2) could recognize the second and third bases as AG or GA, respectively. The loop must also allow the recognition of AA for both factors.

Thus, stop-codon recognition appears to involve elements other than just the tripeptide. Indeed, when a region containing the loop with the tripeptide (residues 163–216 for RF1; 171–226 for RF2) was swapped between RF1 and RF2, both factors were inactive. The tripeptide-swap experiment could only be done in the context of hybrid RFs that contained combinations of residues from RF1 and RF2 in other parts of the molecule (Ito et al., 2000). Therefore, although changing the tripeptide sequence switches stop-codon specificity between RF1 and RF2, it may be that other elements are required to maintain discrimination against the various sense codons.

Peptide Release

A second fundamental problem is how the binding of class I RFs results in peptidyl-tRNA hydrolysis, a reaction that needs to be inhibited during elongation but facilitated during termination. Out of the four class I RF crystal structures solved so far, the GGQ loop is disordered in all except the structure of *E. coli* RF2, where it is constrained by crystal contacts (Vestergaard et al., 2001). However, this loop is ordered in our structures of both RF1 and RF2 (Figures 2B and 2C). The tip of this loop reaches into the PTC, where it faces A76 of P site tRNA and is surrounded by nucleotides C2063, A2451, U2506, and A2602 of 23S RNA (Figure 5). Of these, the closest are A2451 and A2602, the latter being the nucleotide most essential for hydrolysis based on mutational data (Youngman et al., 2004). Notably, the tip of the loop is constituted by not only the GGQ motif but several residues flanking the motif. However, mutational studies have so far focused mainly on the GGQ motif. It is not yet clear whether class I RFs function by directly coordinating a water

(B) $F_o - F_c$ map contoured at 2σ showing RF1 with domains 1 (yellow), 2 (orange) containing the tripeptide "anticodon" PVT (light blue), 3 (red) with the GGQ motif (purple), and 4 (purple-red).

(C) $F_o - F_c$ map contoured at 2σ showing RF2 with domains 1 (dark blue), 2 (slate blue) containing the tripeptide anticodon SPF (pink), 3 (light blue) with the GGQ motif (purple), and 4 (turquoise).

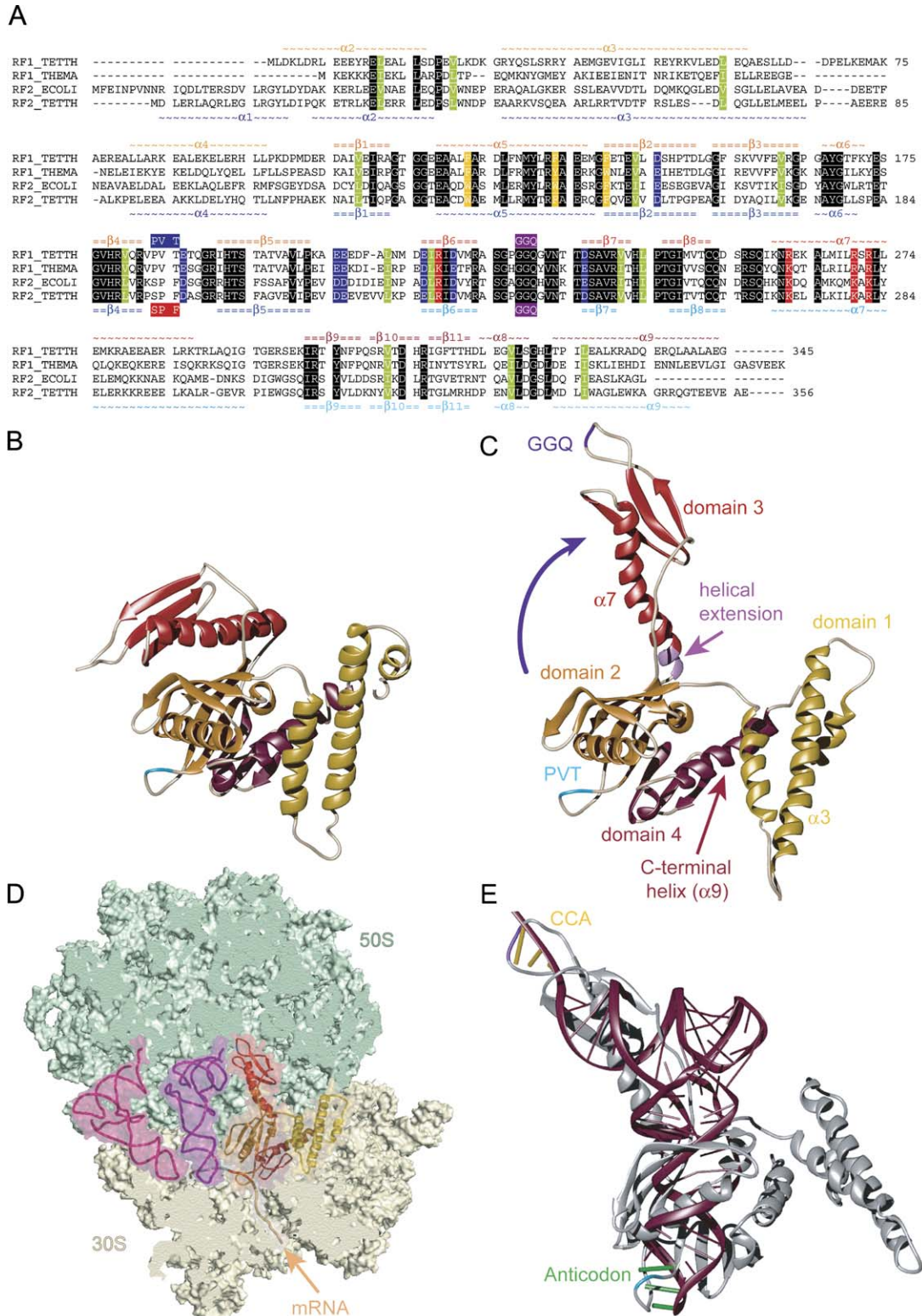


Figure 3. Comparison of Class I RF Structures

Coloring as in Figure 1.

(A) Sequence alignment that was the basis for homology models used to fit the structures of RF1 and RF2 in the electron density maps. (B) Crystal structure of free *T. maritima* RF1 (Shin et al., 2004). The GGQ loop was disordered in this structure.

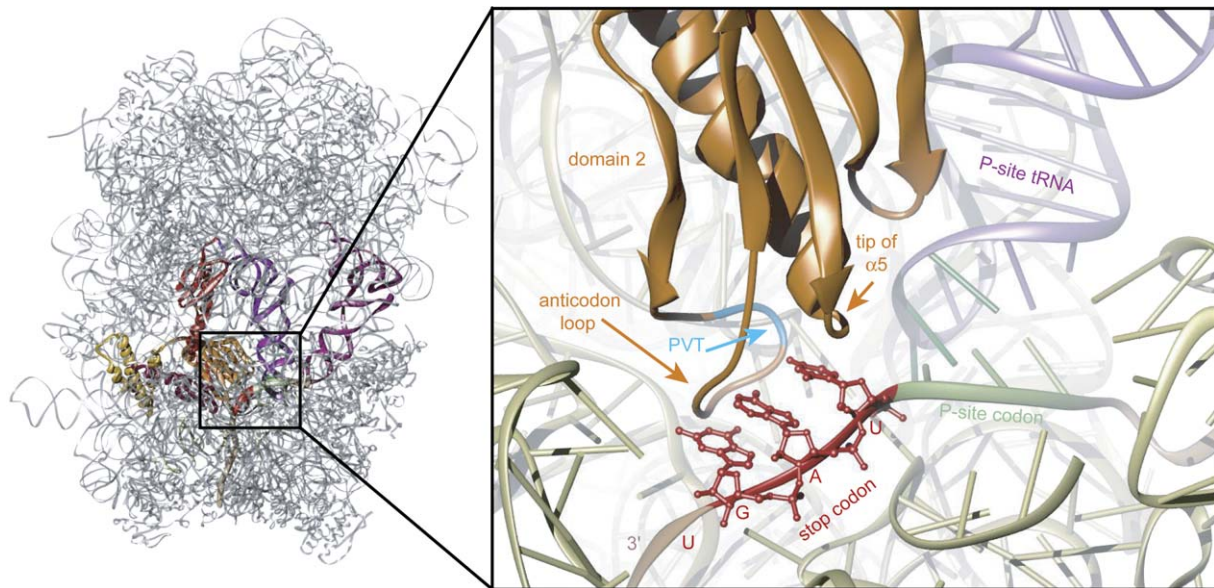


Figure 4. Interaction of RF1 with the Decoding Center of the 30S Subunit, with Overview on the Left and Details on the Right

The stop codon UAG is surrounded by a loop containing a tripeptide (PVT in the case of RF1, shown in light blue), that has been implicated in genetic experiments as conferring specificity for UAG. This loop could not be resolved from its surrounding elements, and its conformation is that of the isolated crystal structure of RF1 (Shin et al., 2004). The tip of helix $\alpha 5$ lies adjacent to the first stop-codon base. The sticks for bases in this and other figures are merely for guidance since base orientations cannot be precisely determined at this resolution.

molecule, as has been proposed (Song et al., 2000), or by inducing conformational changes in the PTC.

Differences between RF1 and RF2

As might be expected given the 50% sequence similarity and the fact that they both perform stop-codon-dependent peptidyl-tRNA hydrolysis, RF1 and RF2 bind to the ribosome in a similar manner. Domains 2, 3, and all but the C-terminal helix of domain 4 assume nearly identical structures in the ribosome ($C\alpha$ rmsd of 2.8 Å between equivalent residues, which is comparable to the typical coordinate error at this resolution; also see Figure S1D). However, domain 1 does assume significantly different conformations in RF1 and RF2. Domain 1 is not directly involved in the release function and has been shown to interact with RF3 (Mora et al., 2003). As discussed below, its interactions with the C-terminal helix are different for RF1 and RF2. This domain shows the largest sequence variation between members of the class I RF family, and, not surprisingly, we find it in significantly different orientations for RF1 and RF2 ($C\alpha$ rmsd of 8.2 Å; also see Figure 6 and Figure S1D).

In RF2, the loop leading into helix $\alpha 3$ and the start of this helix (residues 40–50) are close to nucleotides 1067–1068 of helix 43 and 1095–1096 of helix 44 of the L11 binding region of 23S RNA (Figure 6A). The corresponding part of RF1 (residues 25–33) is shifted away from the L11 binding region by approximately 5 Å, suggesting that it does not directly

contact this region. This finding rationalizes biochemical data suggesting that RF2 interacts with bases 1067 and 1093–1095 (Xu et al., 2002). It also provides a structural basis for the finding that the termination efficiency of RF2 but not RF1 is reduced when bases in the L11 binding region of RNA are mutated.

The differences in the orientation of domain 1 in RF1 and RF2 may arise from differences in the contacts of this domain with the C-terminal helix of domain 4. In RF1, this helix interacts with helices $\alpha 2$ and $\alpha 4$. In the case of RF2, the C-terminal helix associates with $\alpha 1$, $\alpha 3$, and $\alpha 4$ to form a four-helical bundle (Figure S1D).

Strikingly, the N-terminal domain of L11 (L11-NTD) is shifted away from the ribosome when either RF1 or RF2 is bound (Figure 6B). This brings the end of helix $\alpha 2$ of both factors close to residues 21–22 of the proline-rich helix of the L11-NTD (Figure 6C). However, it is not clear at this resolution why the L11-NTD should be necessary for RF1 function but somewhat inhibitory for RF2 (Van Dyke and Murgola, 2003). On the other hand, more recent genetic studies on L11 show that mutations throughout L11 affect RF1 and RF2 function equally (H. Sato, K. Ito, and Y. Nakamura, personal communication), which would be consistent with our observation of a conformational change in L11 with both factors.

The binding site of the thiazole antibiotic thiostrepton has been narrowed down to the region between the L11-NTD and the L11 binding region of 23S RNA (Thompson et al.,

(C) Model of *T. thermophilus* RF1 bound the ribosome.

(D) Cutaway view of RF1 in the ribosome, showing the location of E and P site tRNAs (pink and purple, respectively) and mRNA.

(E) A site tRNA in the ribosome in the same orientation (Yusupov et al., 2001), with the structure of RF1 superimposed in light gray.

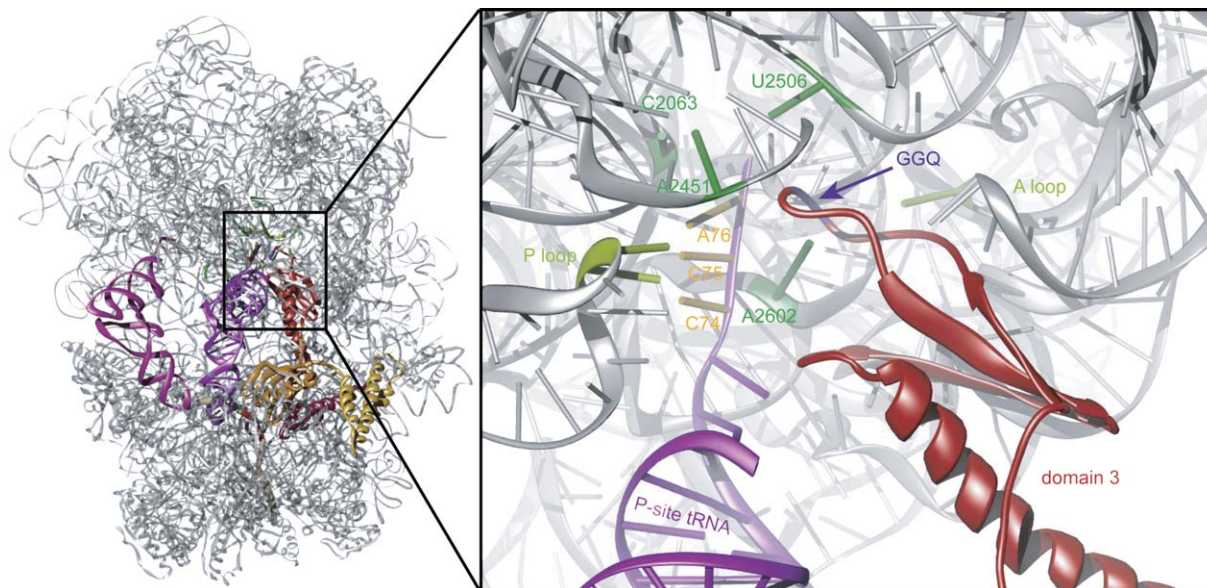


Figure 5. Interaction of RF1 with the Peptidyl Transferase Center of the 50S Subunit and A and P Loops

The highly conserved GGQ loop implicated in peptide release is surrounded by conserved bases of the peptidyl transferase center and faces A76 of P site tRNA.

1979; Ryan et al., 1991). Whereas the C-terminal domain of L11 is closely associated with 23S RNA, the L11-NTD interacts more loosely and has therefore been proposed to function during factor binding as a molecular switch that interacts with translation factors; the binding of thiostrepton would lock the conformation of the L11-NTD, resulting in loss of binding or function of various factors (Wimberly et al., 1999). The movement of the L11-NTD seen in our structures on RF binding and the observation that thiostrepton inhibits class I RF binding (Brot et al., 1974) are consistent with such a role for the L11-NTD. Indeed, movement of the L11-NTD has also been implicated in cryo-EM studies of EF-G binding (Agrawal et al., 2001).

Conclusions

We have shown that it is possible to obtain milligram amounts of homogenous and stable functional complexes of the ribosome at a defined point along the translation pathway and crystallize them. The techniques described here could in principle be used for other states of the ribosome. The structures of the release factors bound to the ribosome expand on prior cryo-EM results and also show details of induced changes within the RFs themselves, such as the ordering of the GGQ loop at the peptidyl transferase center, as well as details of interactions of RF with the PTC and the decoding center. The structures also suggest that the tip of helix $\alpha 5$ of RF may be important for stop-codon recognition. Finally, the structures show a movement of the N-terminal domain of L11 in response to RF binding and differences between RF1 and RF2 in their interaction with this region, which rationalize biochemical and genetic data.

However, a number of fundamental questions remain. Though it is now clear that there is a direct interaction of RFs with the stop codon, we still do not understand the precise structural basis for its recognition and the discrimination against noncognate stop codons as well as sense codons. It is also not clear whether peptide hydrolysis is catalyzed by induced changes in the structure of the PTC, activation of an ordered water molecule, or directly by the class I RFs. Finally, understanding the mechanism of the signaling that results in peptide release in response to stop-codon recognition remains a challenging problem. Progress in these areas will require structures at higher resolution as well as further biochemical and genetic studies.

EXPERIMENTAL PROCEDURES

Ribosomes and mRNA

Thermus thermophilus 70S ribosomes were isolated as described (Clemons et al., 2001), except that a Toyopearl butyl 650S column was used for hydrophobic interaction chromatography and the sucrose-gradient ultracentrifugation was carried out with a zonal rotor with a gradient of 10%–50% sucrose and 10 mM Mg^{2+} in the buffer. Oligonucleotides for the mRNA used for release-complex formation were chemically synthesized and gel purified (Dharmacon). The sequence 5'-pAUGUUC (stop) UACAAUAAU-3', containing either a UAG or UGA stop codon, was designed with a strong 3' termination context as identified with the TransTerm database (Jacobs et al., 2002).

Preparation of tRNA^{Phe}

Overexpression and purification of tRNA^{Phe} was carried out as previously described (Jünemann et al., 1996). The final tRNA was dialyzed against storage buffer (10 mM ammonium acetate [pH 5.0], 50 mM KCl) and stored at $-80^{\circ}C$ in aliquots.

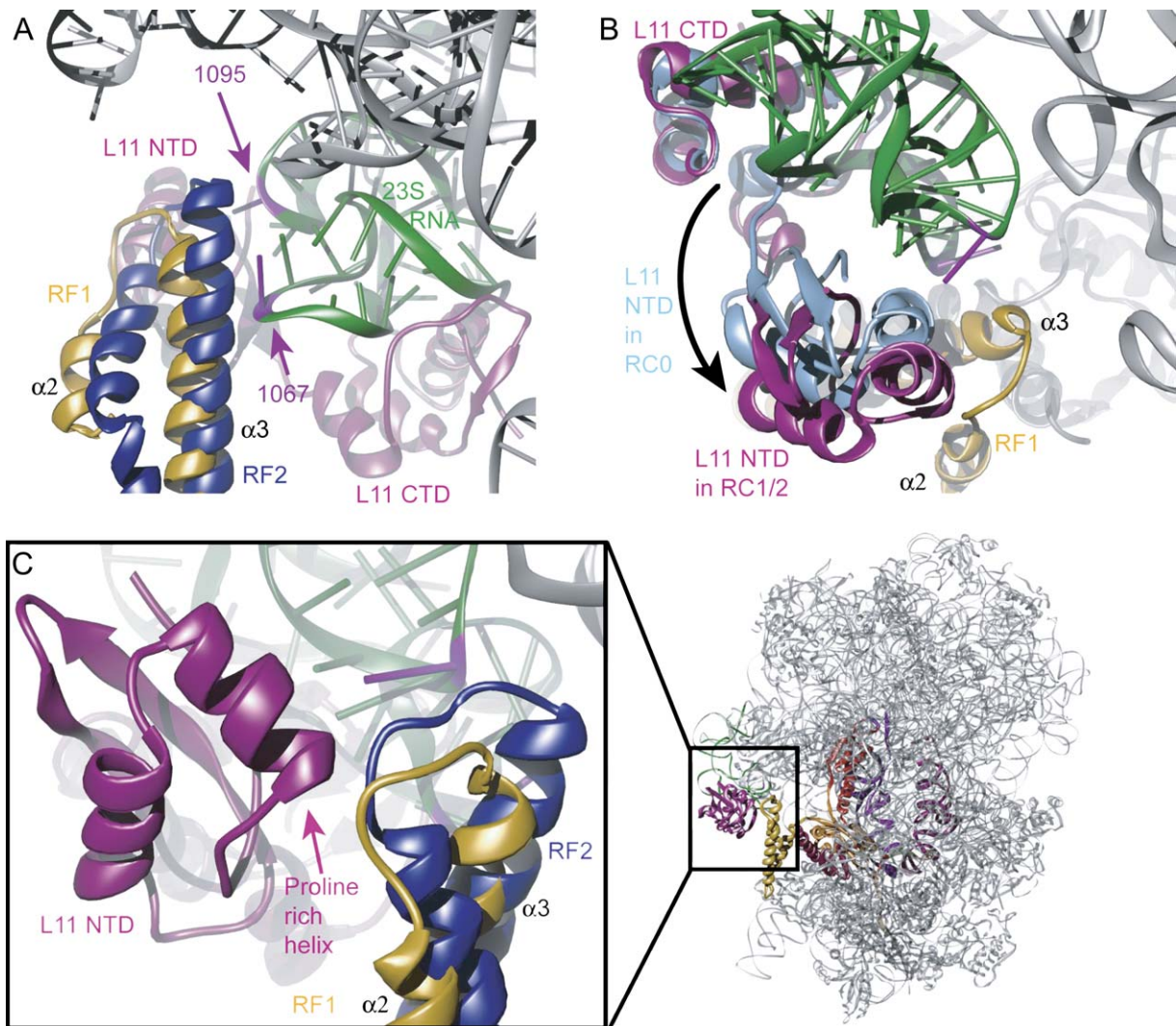


Figure 6. Interaction of RF1 and RF2 with the L11 Region of the Ribosome

(A) Differences between RF1 and RF2. RF2 (blue) is close enough to make direct contact with 23S RNA bases 1067 and 1095 (purple), whereas RF1 (yellow) is about 5 Å further away. No significant change in the RNA conformation between the two structures was observed.

(B) Conformational changes in L11 induced by RF binding. Comparison of the N-terminal domain of L11 when RF is bound (magenta) compared to its conformation without the factor (light blue) shows that the domain appears to be displaced away from the RNA and toward the factors upon RF binding. This is the view from the “top” of the orientation shown in (A).

(C) Close proximity of both RF1 and RF2 to the N-terminal domain of L11, suggesting a direct contact. The orientation shown is that in (A) rotated 90 degrees to the left.

Release Factor Purification

The genes for RF1 and RF2 from *Thermus thermophilus* were cloned with a C-terminal His tag into a pET42bTev vector under the control of a T7 promoter (Studier et al., 1990). pET42bTev is a modified version of pET42b (Novagen) where the factor Xa cleavage site has been exchanged for a Tev protease recognition site. The frameshift required for translation of the natural gene coding for RF2 was avoided by deleting the extraneous sequence during the cloning. After induction and harvesting, the cells were lysed in buffer A (50 mM Na/K phosphate buffer, 300 mM NaCl, 10 mM imidazole, 6 mM 2-mercaptoethanol, 0.1 mM phenylmethylsulfonyl fluoride (PMSF), 0.1 mM DNase I0 [pH 8.0]) using an Emulsiflex cell disruptor. Lysates were incubated at 70°C for 30 min, and the precipitated, endogenous *E. coli* proteins were then removed by centrifugation. RF1 and RF2 were purified from the supernatant by affinity chro-

matography on Ni-NTA agarose (QIAGEN), dialyzed into buffer B (50 mM Tris-Cl, 50 mM KCl, 6 mM 2-mercaptoethanol [pH 8.0]), and further purified on a MonoQ column (Amersham/GE Healthcare; 50–500 mM KCl gradient). After ammonium-sulfate precipitation (50%), the sample was separated by size-exclusion chromatography on a Superdex 75 column (Amersham/GE Healthcare), equilibrated in buffer G (5 mM HEPES, 10 mM MgAc, 50 mM KCl, 10 mM NH₄Cl, 6 mM 2-mercaptoethanol [pH 7.5]), and concentrated to 10 mg/ml for final storage at –80°C.

Release-Complex Formation

Ribosomes (1 μM) were programmed with mRNA (2 μM) and deacylated tRNA^{Phe} (2 μM) by incubation at 55°C for 20 min in buffer G followed by a second incubation step for 10 min in the absence or presence of 5 μM of the appropriate release factor (RF). The release complexes thus

formed (RC1, RC2, or RC0 for complexes with RF1, RF2, or no release factor, respectively) were either directly used (with RC0) or further purified on Ni-NTA agarose columns using the His tag on the RF, with histidine in the elution buffer. Nonspecifically bound ribosomes were eluted at 1 mM histidine, while the ribosomes bound to release factor were eluted with 25 mM histidine. The fraction of ribosomes that eluted with bound release factor was typically 30%–60% of the total. Ribosome complexes were concentrated by ultrafiltration to 4–10 mg/ml and immediately used for crystallization.

Release-Complex Stability and Activity Assay

Stability and occupancy of release complexes were assayed by size-exclusion chromatography on a Superose 6 column (Amersham/GE Healthcare) and SDS-PAGE. The presence of a cognate stop codon (UAG for RF1 or UGA for RF2) in the A site was a requirement for RF binding to the ribosomes as judged by Coomassie-stained SDS gels (see Figure 1).

Peptide-release activity of RFs was measured by the release of tritium-labeled methionine from fMet-tRNA^{fMet} bound to the P site (Caskey et al., 1971). This showed that both RF1 and RF2 are active in a codon-specific manner.

Crystallization

After initial trials and optimization, crystals of the three complexes were grown at 4°C by the vapor diffusion method with a reservoir solution containing 50 mM MES (pH 6.7), 25 mM MgOAc, 200 mM KCl, 75 mM NH₄Cl, PEG20K (2.5%–3.3% for RC1, 2.1%–2.4% for RC2, 3.1%–3.55% for RC0), ethylene glycol (25%–28.5% for RC1, 24%–27% for RC2, 26%–28% for RC0), and 5.8 mM of the detergent deoxy-BIGCHAP (Hampton Research). Crystals were frozen directly from the drop by plunging into liquid nitrogen, and all data collection was carried out at 100 K. The crystals were in the space group P4₃2₁2, with cell dimensions of a = b = 519 Å and c = 365 Å.

Data Collection and Refinement

Crystals were screened at beamline 14.1 at the SRS at Daresbury Laboratory and at beamlines 14-1, 14-2, and 14-3 at ESRF (Grenoble, France). X-ray diffraction data were measured at beamline ID14-4 at ESRF using Strategy (Ravelli et al., 1997) for efficient data collection. Data were integrated and scaled with Denzo and Scalepack (Otwinowski and Minor, 1997). The structure was solved by molecular replacement using CNS (Brünger et al., 1998) with the 30S subunit from *Thermus thermophilus* (Wimberly et al., 2000) and the 50S subunit from *Deinococcus radiodurans* (Harms et al., 2001) as search models. Subsequently, use of an all-atom model of the 70S ribosome from *T. thermophilus* (Jenner et al., 2005) resulted in improved statistics and maps. TLS refinement was carried out with Refmac (Winn et al., 2003), followed by density modification using Solomon (Abrahams and Leslie, 1996). F_o – F_c electron density maps were calculated from observed structure-factor amplitudes measured from RC1 or RC2 and the factorless RC, using the density-modified phases. These maps were used to build the release-factor domains since they gave the most continuous density for the factor. This is probably because scaling of F_o to F_c at this resolution is not particularly accurate owing to solvent contributions to the structure factor. For F_o – F_c maps, the maps that appeared best visually were obtained using CNS (Brünger et al., 1998) with phases from rigid-body refinement, initially of the whole subunits, then of large domains of each subunit, and finally of a large number of domains consisting of individual stem loops and proteins, followed by grouped B factor refinement in which each rigid-body domain was treated as a single group. The CCP4 suite of programs was used throughout for various routine tasks (CCP4, 1994).

Modeling

Models were built using O (Jones and Kjeldgaard, 1997), and figures were made using Ribbons (Carson, 1991). Homology models of *T. thermophilus* RF1 and RF2 were obtained using Swiss Model and the “merge atom” function of O with crystals structures of *T. maritima* RF1 (Shin et al., 2004) and *E. coli* RF2 (Vestergaard et al., 2001) as templates. Both RF models

were docked into electron density manually by first keeping the domain structure intact while moving around hinge regions and then adjusting helices that were clearly in a different conformation. The final RF structures were subjected to several rounds of conjugate-gradient energy minimization and rigid-body refinement using CNS (Brünger et al., 1998). A site tRNA from the 5.5 Å structure of the 70S ribosome from *T. thermophilus* (1GIX; Yusupov et al., 2001) was superimposed onto the current crystal structure. The crystal structure of tRNA^{Phe} (1E1Y; Goldgur et al., 1997) was used to model E site tRNA. The P site bound tRNA^{Phe} observed previously in complex with the ribosome (Jenner et al., 2005) was adjusted at its CCA end to fit the density. The L1 and L7/L12 regions were removed from the final model because the lack of interpretable density for either indicated that they were disordered.

Supplemental Data

Supplemental Data include Supplemental References and one figure and can be found with this article online at <http://www.cell.com/cgi/content/full/123/7/1255/DC1/>.

ACKNOWLEDGMENTS

We thank Raimond Ravelli, Sean McSweeney, and Gordon Leonard for their help and advice at the ESRF beamlines; Garib Murshudov and Paul Adams for help and advice with the programs REFMAC and CNS, respectively; Albert Weixlbaumer and John Weir for help with synchrotron data collection; and Lori Passmore and T. Martin Schmeing for critical comments. This work was supported by the Medical Research Council (UK), NIH grant GM67624, and a grant from the Agouron Institute. S.P. is supported by a Boehringer-Ingelheim fellowship, C.M.D. is supported by an American Cancer Society Postdoctoral Fellowship, and M.S. is supported by a Wenner-Gren fellowship.

Received: August 17, 2005

Revised: September 20, 2005

Accepted: September 27, 2005

Published: December 28, 2005

REFERENCES

- Abrahams, J.P., and Leslie, A.G.W. (1996). Methods used in the structure determination of bovine mitochondrial F1 ATPase. *Acta Crystallogr. D* 52, 30–42.
- Agrawal, R.K., Linde, J., Sengupta, J., Nierhaus, K.H., and Frank, J. (2001). Localization of L11 protein on the ribosome and elucidation of its involvement in EF-G-dependent translocation. *J. Mol. Biol.* 311, 777–787.
- Arkov, A.L., and Murgola, E.J. (1999). Ribosomal RNAs in translation termination: facts and hypotheses. *Biochemistry (Mosc.)* 64, 1354–1359.
- Arkov, A.L., Freistroffer, D.V., Ehrenberg, M., and Murgola, E.J. (1998). Mutations in RNAs of both ribosomal subunits cause defects in translation termination. *EMBO J.* 17, 1507–1514.
- Brot, N., Tate, W.P., Caskey, C.T., and Weissbach, H. (1974). The requirement for ribosomal proteins L7 and L12 in peptide-chain termination. *Proc. Natl. Acad. Sci. USA* 71, 89–92.
- Brünger, A.T., Adams, P.D., Clore, G.M., DeLano, W.L., Gros, P., Grosse-Kunstleve, R.W., Jiang, J.S., Kuszewski, J., Nilges, M., Pannu, N.S., et al. (1998). Crystallography & NMR system: A new software suite for macromolecular structure determination. *Acta Crystallogr. D Biol. Crystallogr.* 54, 905–921.
- Capecchi, M.R. (1967). Polypeptide chain termination in vitro: isolation of a release factor. *Proc. Natl. Acad. Sci. USA* 58, 1144–1151.
- Carson, M. (1991). Ribbons 2.0. *J. Appl. Crystallogr.* 24, 958–961.
- Caskey, C.T., Tompkins, R., Scolnick, E., Caryk, T., and Nirenberg, M. (1968). Sequential translation of trinucleotide codons for the initiation and termination of protein synthesis. *Science* 162, 135–138.

- Caskey, C.T., Beaudet, A.L., Scolnick, E.M., and Rosman, M. (1971). Hydrolysis of fMet-tRNA by peptidyl transferase. *Proc. Natl. Acad. Sci. USA* 68, 3163–3167.
- Cate, J.H., Yusupov, M.M., Yusupova, G.Z., Earnest, T.N., and Noller, H.F. (1999). X-ray crystal structures of 70S ribosome functional complexes. *Science* 285, 2095–2104.
- Clemons, W.M., Jr., Brodersen, D.E., McCutcheon, J.P., May, J.L., Carter, A.P., Morgan-Warren, R.J., Wimberly, B.T., and Ramakrishnan, V. (2001). Crystal structure of the 30S ribosomal subunit from *Thermus thermophilus*: purification, crystallization and structure determination. *J. Mol. Biol.* 310, 827–843.
- CCP4 (Collaborative Computational Project Number 4) (1994). The CCP4 suite: programs for protein crystallography. *Acta Crystallogr. D Biol. Crystallogr.* 50, 760–763.
- Dincbas-Renqvist, V., Engstrom, A., Mora, L., Heurgue-Hamard, V., Buckingham, R., and Ehrenberg, M. (2000). A post-translational modification in the GGQ motif of RF2 from *Escherichia coli* stimulates termination of translation. *EMBO J.* 19, 6900–6907.
- Freistroffer, D.V., Kwiatkowski, M., Buckingham, R.H., and Ehrenberg, M. (2000). The accuracy of codon recognition by polypeptide release factors. *Proc. Natl. Acad. Sci. USA* 97, 2046–2051.
- Frolova, L.Y., Tsvikovskii, R.Y., Sivolobova, G.F., Oparina, N.Y., Serpinsky, O.I., Blinov, V.M., Tatkov, S.I., and Kisselev, L.L. (1999). Mutations in the highly conserved GGQ motif of class 1 polypeptide release factors abolish ability of human eRF1 to trigger peptidyl-tRNA hydrolysis. *RNA* 5, 1014–1020.
- Goldgur, Y., Mosyak, L., Reshetnikova, L., Ankilova, V., Lavrik, O., Khodyreva, S., and Safran, M. (1997). The crystal structure of phenylalanyl-tRNA synthetase from *Thermus thermophilus* complexed with cognate tRNA^{Phe}. *Structure* 5, 59–68.
- Harms, J., Schlutzenzen, F., Zarivach, R., Bashan, A., Gat, S., Agmon, I., Bartels, H., Franceschi, F., and Yonath, A. (2001). High resolution structure of the large ribosomal subunit from a mesophilic eubacterium. *Cell* 107, 679–688.
- Heurgue-Hamard, V., Champ, S., Mora, L., Merkoulouva-Rainon, T., Kisselev, L.L., and Buckingham, R.H. (2005). The glutamine residue of the conserved GGQ motif in *Saccharomyces cerevisiae* release factor eRF1 is methylated by the product of the YDR140w gene. *J. Biol. Chem.* 280, 2439–2445.
- Ito, K., Uno, M., and Nakamura, Y. (1998). Single amino acid substitution in prokaryote polypeptide release factor 2 permits it to terminate translation at all three stop codons. *Proc. Natl. Acad. Sci. USA* 95, 8165–8169.
- Ito, K., Uno, M., and Nakamura, Y. (2000). A tripeptide “anticodon” deciphers stop codons in messenger RNA. *Nature* 403, 680–684.
- Jacobs, G.H., Rackham, O., Stockwell, P.A., Tate, W., and Brown, C.M. (2002). TransTerm: a database of mRNAs and translational control elements. *Nucleic Acids Res.* 30, 310–311.
- Jenner, L., Romy, P., Rees, B., Schulze-Briese, C., Springer, M., Ehresmann, C., Ehresmann, B., Moras, D., Yusupova, G., and Yusupov, M. (2005). Translational operator of mRNA on the ribosome: how repressor proteins exclude ribosome binding. *Science* 308, 120–123.
- Jones, T.A., and Kjeldgaard, M. (1997). Electron-density map interpretation. *Methods Enzymol.* 277, 173–208.
- Jünemann, R., Wadzack, J., Triana-Alonso, F.J., Bittner, J.U., Caillet, J., Meinel, T., Vanatalu, K., and Nierhaus, K.H. (1996). In vivo deuteration of transfer RNAs: overexpression and large-scale purification of deuterated specific tRNAs. *Nucleic Acids Res.* 24, 907–913.
- Klaholz, B.P., Pape, T., Zavialov, A.V., Myashnikov, A.G., Orlova, E.V., Vestergaard, B., Ehrenberg, M., and van Heel, M. (2003). Structure of the *Escherichia coli* ribosomal termination complex with release factor 2. *Nature* 421, 90–94.
- Konecki, D.S., Aune, K.C., Tate, W., and Caskey, C.T. (1977). Characterization of reticulocyte release factor. *J. Biol. Chem.* 252, 4514–4520.
- Mora, L., Zavialov, A., Ehrenberg, M., and Buckingham, R.H. (2003). Stop codon recognition and interactions with peptide release factor RF3 of truncated and chimeric RF1 and RF2 from *Escherichia coli*. *Mol. Microbiol.* 50, 1467–1476.
- Mottagui-Tabar, S. (1998). Quantitative analysis of in vivo ribosomal events at UGA and UAG stop codons. *Nucleic Acids Res.* 26, 2789–2796.
- Otwinowski, Z., and Minor, W. (1997). Processing of X-ray diffraction data collected in oscillation mode. *Methods Enzymol.* 276, 307–326.
- Polacek, N., Gomez, M.J., Ito, K., Xiong, L., Nakamura, Y., and Mankin, A. (2003). The critical role of the universally conserved A2602 of 23S ribosomal RNA in the release of the nascent peptide during translation termination. *Mol. Cell* 11, 103–112.
- Poole, E.S., Brown, C.M., and Tate, W.P. (1995). The identity of the base following the stop codon determines the efficiency of in vivo translational termination in *Escherichia coli*. *EMBO J.* 14, 151–158.
- Ravelli, R.B.G., Sweet, R.M., Skinner, J.M., Duisenberg, A.J.M., and Kroon, J. (1997). STRATEGY: a program to optimize the starting spindle angle and scan range for X-ray data collection. *J. Appl. Crystallogr.* 30, 551–554.
- Rawat, U.B., Zavialov, A.V., Sengupta, J., Valle, M., Grassucci, R.A., Linde, J., Vestergaard, B., Ehrenberg, M., and Frank, J. (2003). A cryo-electron microscopic study of ribosome-bound termination factor RF2. *Nature* 421, 87–90.
- Ryan, P.C., Lu, M., and Draper, D.E. (1991). Recognition of the highly conserved GTPase center of 23S ribosomal RNA by ribosomal protein L11 and the antibiotic thiostrepton. *J. Mol. Biol.* 221, 1257–1268.
- Scolnick, E., Tompkins, R., Caskey, T., and Nirenberg, M. (1968). Release factors differing in specificity for terminator codons. *Proc. Natl. Acad. Sci. USA* 61, 768–774.
- Seit-Nebi, A., Frolova, L., Justesen, J., and Kisselev, L. (2001). Class-1 translation termination factors: invariant GGQ minidomain is essential for release activity and ribosome binding but not for stop codon recognition. *Nucleic Acids Res.* 29, 3982–3987.
- Shin, D.H., Brandsen, J., Jancarik, J., Yokota, H., Kim, R., and Kim, S.H. (2004). Structural analyses of peptide release factor 1 from *Thermotoga maritima* reveal domain flexibility required for its interaction with the ribosome. *J. Mol. Biol.* 341, 227–239.
- Song, H., Mugnier, P., Das, A.K., Webb, H.M., Evans, D.R., Tuite, M.F., Hemmings, B.A., and Barford, D. (2000). The crystal structure of human eukaryotic release factor eRF1—mechanism of stop codon recognition and peptidyl-tRNA hydrolysis. *Cell* 100, 311–321.
- Stark, H., Rodnina, M.V., Wieden, H.J., Zemlin, F., Wintermeyer, W., and Van Heel, M. (2002). Ribosome interactions of aminoacyl-tRNA and elongation factor Tu in the codon-recognition complex. *Nat. Struct. Biol.* 9, 849–854.
- Studier, F.W., Rosenberg, A.H., Dunn, J.J., and Dubendorff, J.W. (1990). Use of T7 RNA polymerase to direct expression of cloned genes. *Methods Enzymol.* 185, 61–89.
- Tate, W., Schulze, H., and Nierhaus, K. (1983). The *Escherichia coli* ribosomal protein L11 suppresses release factor 2 but promotes the release factor 1 activities in peptide chain termination. *J. Biol. Chem.* 258, 12816–12820.
- Thompson, J., Cundliffe, E., and Stark, M. (1979). Binding of thiostrepton to a complex of 23-S rRNA with ribosomal protein L11. *Eur. J. Biochem.* 98, 261–265.
- Uno, M., Ito, K., and Nakamura, Y. (2002). Polypeptide release at sense and noncognate stop codons by localized charge-exchange alterations in translational release factors. *Proc. Natl. Acad. Sci. USA* 99, 1819–1824.
- Valle, M., Sengupta, J., Swami, N.K., Grassucci, R.A., Burkhardt, N., Nierhaus, K.H., Agrawal, R.K., and Frank, J. (2002). Cryo-EM reveals an

- active role for aminoacyl-tRNA in the accommodation process. *EMBO J.* *21*, 3557–3567.
- Van Dyke, N., and Murgola, E.J. (2003). Site of functional interaction of release factor 1 with the ribosome. *J. Mol. Biol.* *330*, 9–13.
- Van Dyke, N., Xu, W., and Murgola, E.J. (2002). Limitation of ribosomal protein L11 availability in vivo affects translation termination. *J. Mol. Biol.* *319*, 329–339.
- Vestergaard, B., Van, L.B., Andersen, G.R., Nyborg, J., Buckingham, R.H., and Kjeldgaard, M. (2001). Bacterial polypeptide release factor RF2 is structurally distinct from eukaryotic eRF1. *Mol. Cell* *8*, 1375–1382.
- Wimberly, B.T., Guymon, R., McCutcheon, J.P., White, S.W., and Ramakrishnan, V. (1999). A detailed view of a ribosomal active site: the structure of the L11- RNA complex. *Cell* *97*, 491–502.
- Wimberly, B.T., Brodersen, D.E., Clemons, W.M., Jr., Morgan-Warren, R.J., Carter, A.P., Vornrhein, C., Hartsch, T., and Ramakrishnan, V. (2000). Structure of the 30S ribosomal subunit. *Nature* *407*, 327–339.
- Winn, M.D., Murshudov, G.N., and Papiz, M.Z. (2003). Macromolecular TLS refinement in REFMAC at moderate resolutions. *Methods Enzymol.* *374*, 300–321.
- Xu, W., Pagel, F.T., and Murgola, E.J. (2002). Mutations in the GTPase center of Escherichia coli 23S rRNA indicate release factor 2-interactive sites. *J. Bacteriol.* *184*, 1200–1203.
- Youngman, E.M., Brunelle, J.L., Kochaniak, A.B., and Green, R. (2004). The active site of the ribosome is composed of two layers of conserved nucleotides with distinct roles in peptide bond formation and peptide release. *Cell* *117*, 589–599.
- Yusupov, M.M., Yusupova, G.Z., Baucom, A., Lieberman, K., Earnest, T.N., Cate, J.H.D., and Noller, H.F. (2001). Crystal structure of the ribosome at 5.5 Å resolution. *Science* *292*, 883–896.
- Zavialov, A.V., Buckingham, R.H., and Ehrenberg, M. (2001). A posttermination ribosomal complex is the guanine nucleotide exchange factor for peptide release factor rf3. *Cell* *107*, 115–124.
- Zavialov, A.V., Mora, L., Buckingham, R.H., and Ehrenberg, M. (2002). Release of peptide promoted by the GGQ motif of class 1 release factors regulates the GTPase activity of RF3. *Mol. Cell* *10*, 789–798.

Accession Numbers

Coordinates and structure factors for the three complexes have been deposited in the Protein Data Bank with ID codes 2B9O and 2B9P (RC0), 2B64 and 2B66 (RC1), and 2B9M and 2B9N (RC2).

Supplemental Data

Crystal Structures of the Ribosome in Complex with Release Factors RF1 and RF2 Bound to a Cognate Stop Codon

**Sabine Petry, Ditlev E. Brodersen, Frank V. Murphy IV, Christine M. Dunham,
Maria Selmer, Michael J. Tarry, Ann C. Kelley, and V. Ramakrishnan**

Supplemental References

Klaholz, B. P., Pape, T., Zavialov, A. V., Myasnikov, A. G., Orlova, E. V., Vestergaard, B., Ehrenberg, M., and van Heel, M. (2003). Structure of the Escherichia coli ribosomal termination complex with release factor 2. *Nature* *421*, 90-94.

Rawat, U. B., Zavialov, A. V., Sengupta, J., Valle, M., Grassucci, R. A., Linde, J., Vestergaard, B., Ehrenberg, M., and Frank, J. (2003). A cryo-electron microscopic study of ribosome-bound termination factor RF2. *Nature* *421*, 87-90.

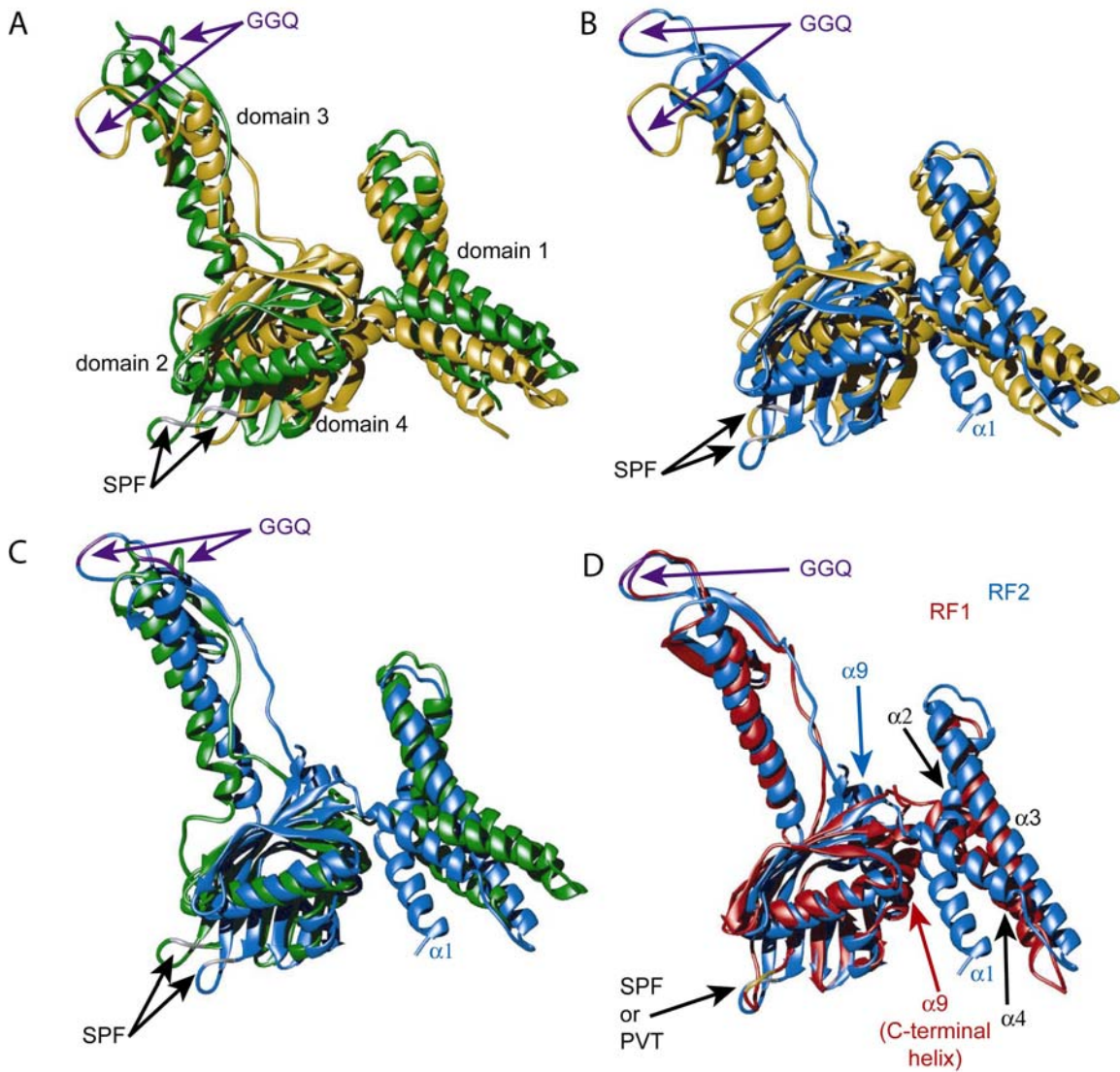


Figure S1. Comparison of Class I RF Models in the Ribosome

(A) Cryo-EM models of RF2 from Klaholz et al. (2003) (yellow) and Rawat et al. (2003) (green).

(B) Crystal structure of *T. thermophilus* RF2 (blue) versus cryo-EM model of Klaholz et al. (2003) (yellow). In (B) and (C), common elements of the ribosome in the pairs of coordinates were used for a least-squares superposition.

(C) Crystal structure of *T. thermophilus* RF2 (blue) versus cryo-EM model of Rawat et al. (2003) (green)

(D) Superposition of the crystal structures of RF1 (red) and RF2 (blue).